



An improved deep learning procedure for statistical downscaling of climate data

Ahmed M.S. Kheir^{a,b,*}, Abdelrazek Elnashar^c, Alaa Mosad^{a,b}, Ajit Govind^a

^a International Center for Agricultural Research in the Dry Areas (ICARDA), Maadi 11728, Egypt

^b Soils, Water and Environment Research Institute, Agricultural Research Center, 9 Cairo University Street, Giza 12112, Egypt

^c Department of Natural Resources, Faculty of African Postgraduate Studies, Cairo University, Giza 12613, Egypt

ARTICLE INFO

Keywords:

Climate change scenarios

GCM

SSP

Convolutional neural network

Bias adjustment

Standardization

ABSTRACT

Recent climate change (CC) scenarios from the Coupled Model Intercomparison Project Phase 6 (CMIP6) have just been released in coarse resolution. Deep learning (DL) based on statistical downscaling has recently been used, but more research is needed, particularly in arid regions, because little is known about their suitability for extrapolating future CC scenarios. Here we analyzed this issue by downscaling maximum, and minimum temperature over the Egyptian domain based on one General Circulation Model (GCM) as CanESM5 and two shared socio-economic pathways (SSPs) as SSP4.5 and SSP8.5 using Convolutional Neural Network (CNN) herein after called CNNSD. The downscaled maximum and minimum temperatures based CNNSD was able to reproduce the observed climate over historical and future periods at a finer resolution (0.1°), reducing the biases exhibited by the original scenario. To the best of our knowledge, this is the first time CNN has been used to downscale CMIP6 scenarios, particularly in arid regions. The downscaled analysis showed that maximum and minimum temperatures are expected to rise by 4.8 °C and 4.0 °C, respectively, in the future (2015–2100), compared to the historical period, under the moderate scenario (SSP4.5). Meanwhile, under the Fossil-fueled Development scenario (SSP8.5), these values will rise by 6.3 °C and 4.2 °C, respectively as analyzed by the CNNSD. The developed approach could be used not only in Egypt but also in other developing countries, which are especially vulnerable to climate change and has a scarcity of related research. The established downscaled approach's supply can be used to provide climate services, as a driver for impact studies and adaptation decisions, and as information for policy development. More research is needed, however, to include multi-GCMs to quantify the uncertainties between GCMs and SSPs, improving the outputs for use in climate change impacts and adaptations for food and nutrition security.

1. Introduction

Climate change is harming global food and nutrition security, and it is expected to worsen [1–4]. We need to study recent climate scenarios at acceptable temporal and spatial resolutions to quantify the impacts of climate change [5], and governance of agricultural systems in changing climate conditions [6,7]. The latest Coupled Model Intercomparison Project (CMIP) scenarios are the fifth phase of CMIP (CMIP5) at 200 km spatial resolutions [8,9] and the sixth phase of CMIP (CMIP6) at 100 km spatial resolutions [10]. The CMIP

* Corresponding author. International Center for Agricultural Research in the Dry Areas (ICARDA), Maadi 11728, Egypt.

E-mail addresses: a.kheir@cgiar.org, drahmedkheir2015@gmail.com (A.M.S. Kheir).

<https://doi.org/10.1016/j.heliyon.2023.e18200>

Received 2 March 2023; Received in revised form 11 July 2023; Accepted 11 July 2023

Available online 20 July 2023

2405-8440/© 2023 The Authors. Published by Elsevier Ltd. This is an open access article under the CC BY-NC-ND license (<http://creativecommons.org/licenses/by-nc-nd/4.0/>).

initiative uses general circulation models (GCMs) to periodically develop multi-model ensembles of centennial global climate projections under various scenarios [11].

CMIP has been widely used in global studies for instance change of monsoon [12], offshore wind energy resources [13], projections of crop yield [14], precipitation simulation [15–17], mean sea-level change and sea surface temperature [18,19], and simulation of land surface air temperature [20], projections portrayed the recently observed warming [21]. It is also widely used in regional and continental studies for example simulation of climatological temperature and precipitation for Southeast Asia [22], characteristics of future drought over South Asia [23], simulations of extreme precipitation over the USA [24], simulations of evapotranspiration across Africa [25]. However, the spatial resolution of CMIP's latest phase is 100 km, which could fail to capture the detailed patterns, particularly on the national scale. Hence CMIP6 spatial resolution still need to be improved for better environmental studies, confirming the significance of the current study which for sure helps to achieve climate-related sustainable development goals [26,27].

Spatiotemporal statistical downscaling is an effective way to obtain fine-resolution data. This method is based on building a correlation function between a predictand (e.g., temperature) and environmental variables (predictors), and then using the finer predictors as input to downscale the predictand from coarse resolution to fine resolution [28–30]. Previous studies have proved that the downscaled products affected the environmental model when forced with the downscaled data [e.g., 31, 32, 33]. Herein, the correlation function can be built using multiple linear regression [34,35], machine learning [28,36], and deep learning [37,38]. Recently, the magnitude of the maximum and minimum temperatures for the near and middle decades was predicted using the statistical downscaling climate projection model (SimCLIM) [7,39,40]. Similar studies were conducted over Asia to downscale temperatures [41] and precipitation [42,43] using different linear regression models. Deep learning methods should be studied further because they can find patterns in massive unstructured data sets using highly complicated neural networks that imitate the way the human brain functions. In this situation, deep learning can assure complicated nonlinear relationships and solve problems that regular machine learning models cannot. Deep learning based on convolutional neural networks (CNN) has recently been used among these techniques [44,45], because of its capacity to automatically choose predictors in the form of data-riven spatial features [46]. However, the application of these methods, particularly deep learning with CMIP6 scenarios, has received less attention thus far, especially in arid regions. Therefore, this study is focusing on the spatiotemporal statistical downscaling of temperature from CMIP6 over Egypt using deep learning for the first time. To our knowledge, this is the first national-scale temperature dataset produced using deep learning downscaling methods in the study area. The results of this study could help achieve climate-related sustainable development goals.

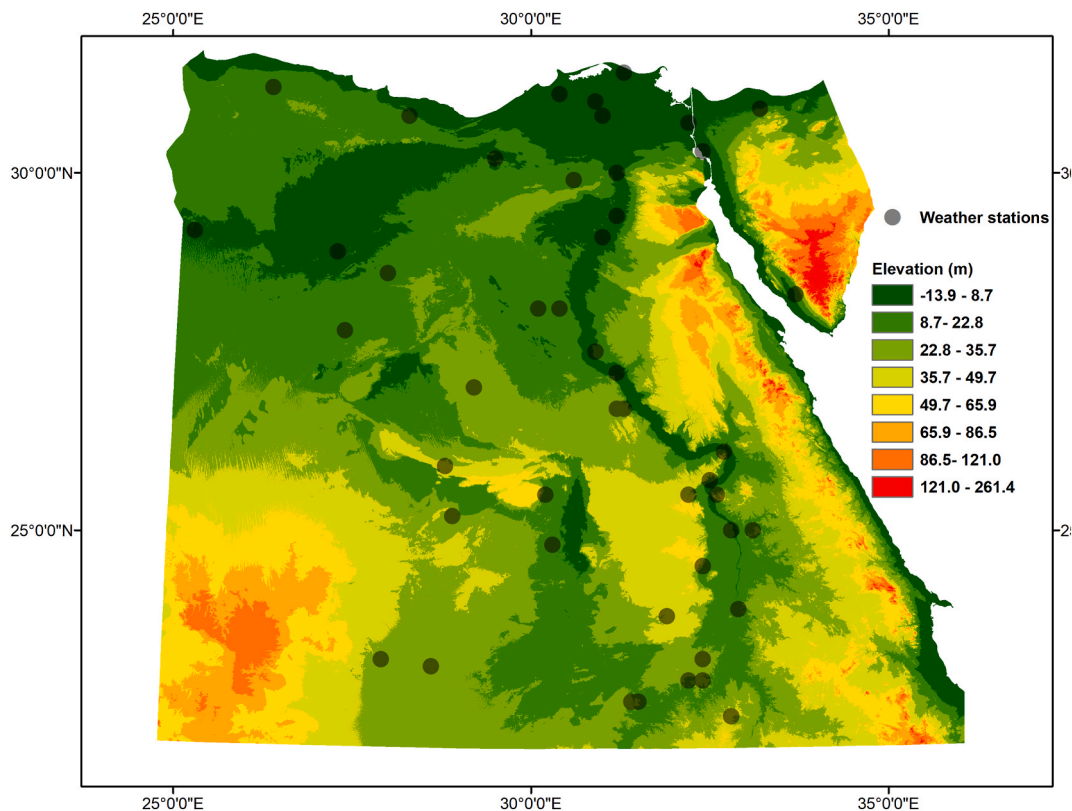


Fig. 1. Map of the study region with digital elevation model (m) and weather stations for the observed dataset.

2. Dataset and methods

2.1. Study region

The research was carried out in Egypt, which has a land area of 1,002,450 km² and is the world's 29th largest country (Fig. 1). Egypt's coordinates are between latitudes 22° and 31° North, which means that the cancer orbit passes through the country's southern part, passing through Aswan city, and between longitudes 24° and 37° East of Greenwich. Egypt, a largely desert and hyper-arid region, is in one of the world's most environmentally vulnerable areas. In the context of global warming, the country became a hotspot for climatic extremes and aridity change [47]. We, therefore, selected maximum and minimum temperatures in CMIP6 scenarios for downscaling from coarse (200 km) to fine resolution (10 km).

2.2. Dataset

Observed climatic data of daily maximum and minimum temperatures (1980–2014) were collected from NASA power at 1° resolution and corrected from some energy balance stations in Egypt (Supplementary Fig. 1). This dataset was spatially interpolated to a finer resolution of 10 km and used as predictands in training the CNN model. In addition to the observed dataset, the CNN model was trained over the historical period (1980–2014) using the ERA5 global reanalysis (50 km) [48], following the perfect prognosis approach [49]. This entails finding empirical correlations between reanalysis parameters of interest for surface weather at high spatial resolution, such as circulation fields, temperature, and humidity. The learned model is directly transferable to different driving GCMs, which is the key benefit of perfect prognosis. This is predicated on the perfect prognosis supposition that the statistical traits and associations produced from reanalysis fields during the training stage are a good approximation of those out-of-sample traits and connections (i.e., provided by other driving GCMs). The predictors used in model training and their units included air temperature (k), specific humidity (g kg⁻¹), geopotential height (m), meridional wind velocity (m s⁻¹), zonal wind velocity (m s⁻¹), and vertical wind velocity (m s⁻¹) at 850 hPa creating a total of 6 variables per grid box. Daily climatic data for selected variables in the historical (1980–2014) were downloaded from ERA 5 reanalysis, while future GCM at near-term (2015–2050), mid-term (2050–2075), and late-term time series (2075–2100) were downloaded from ESGF. Under one Global Climate model (GCM), Canadian Center for Climate Modeling and Analysis (CanESM5) include two shared socioeconomic pathways (SSPs) such as moderate scenario (SSP4.5) and a business-as-usual scenario (SSP8.5) were chosen.

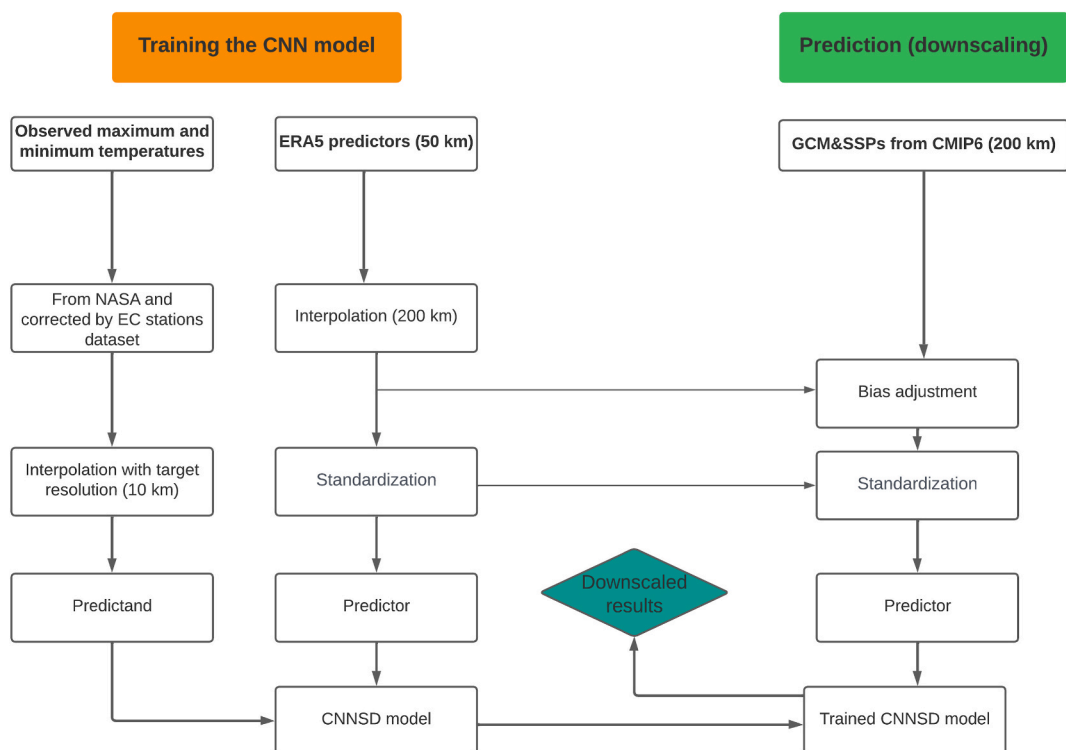


Fig. 2. Preprocessing method workflow and steps for downscaling CMIP6 scenarios using convolutional neural network algorithm.

2.3. Data preprocessing and statistical downscaling based on the CNN model

Deep learning (DL) is an improved version of an artificial neural network inspired by the human brain that effectively analyses massive volumes of data to uncover patterns and characteristics. Recently, the performance of DL models in imaging areas has been demonstrated, and Convolutional Neural Network (CNN) is extensively used deep learning models [50,51]. To discover the features of the data, CNN multiplies by sliding the kernel at the position of the input data, totaling the values, and summarizing them into a single value [52,53]. This procedure is used to extract the data's elements. The CNN models are typically applied to two-dimensional arrays such as image data. However, CNN can also be used to analyze regression data. In this case, we use a one-dimensional convolutional network to reshape the input data. The Keras as a high-level neural network library that runs on top of TensorFlow, includes the Conv1D class, which allows you to add a one-dimensional convolutional layer to your model [54]. We developed CNN after [37,38], which was trained over the period 1980–2014 using daily predictors at 50 km resolution from ERA5, and predictands at 10 km resolution (Fig. 2). Three layers of convolutions (50:25:10), each constructed by three 3×3 spatial kernels, are fed by an input layer (with stacked spatial predictors) in CNN. Using linear transformations, the final convolution is fully connected to the output layer (observed dataset). Given the predictors, the networks are trained to learn conditional daily distributions of maximum and minimum temperatures (minimizing the mean square error, MSE); in other words, the network is compelled to estimate the corresponding parameters to the distributions indicated. We reduce the MSE, which is like reducing the conditional mean's negative log-likelihood from a Gaussian distribution.

The effective handling of intricate spatial elements is where CNN topologies' potential lies. These models can handle high-dimensional predictor spaces while downscaling the climate, choosing the variables and geographic domains that affect each specific site automatically [55,56]. This is important since modern SD approaches, like well-established generalized linear models (GLMs), cannot handle this high dimensionality without overfitting, necessitating, in most cases, some sort of human-guided feature selection (with the ensuing loss of pertinent information).

In this study, we tested the CNN model using a high-dimensional input grid and various predictors like those examined by Refs. [37, 55]. We trained the CNN model using predictors from the historical period and the observed dataset of maximum and minimum temperatures at the same time at high resolution (10 km) (Fig. 2). The projections from these scenarios were then downscaled for the historical (1980–2014) and SSPs (2015–2100) periods using our trained models. We prepared bias adjustment and standardization for the future predictors with the corresponding reanalysis values to assure they reasonably resemble the historical variables used to train the CNNSD model. In addition, we used a change-preserving technique to prevent adding unnatural trends or changes to future scenarios [57]. We employ a distributional downscaling strategy, just like Bao-Medina et al. (2020), and employ the network to estimate daily predictor-conditioned Gaussian distributions. To do early stopping and halt training when the test error stops dropping after 25 epochs, we create a test set by randomly selecting 20% of the data.

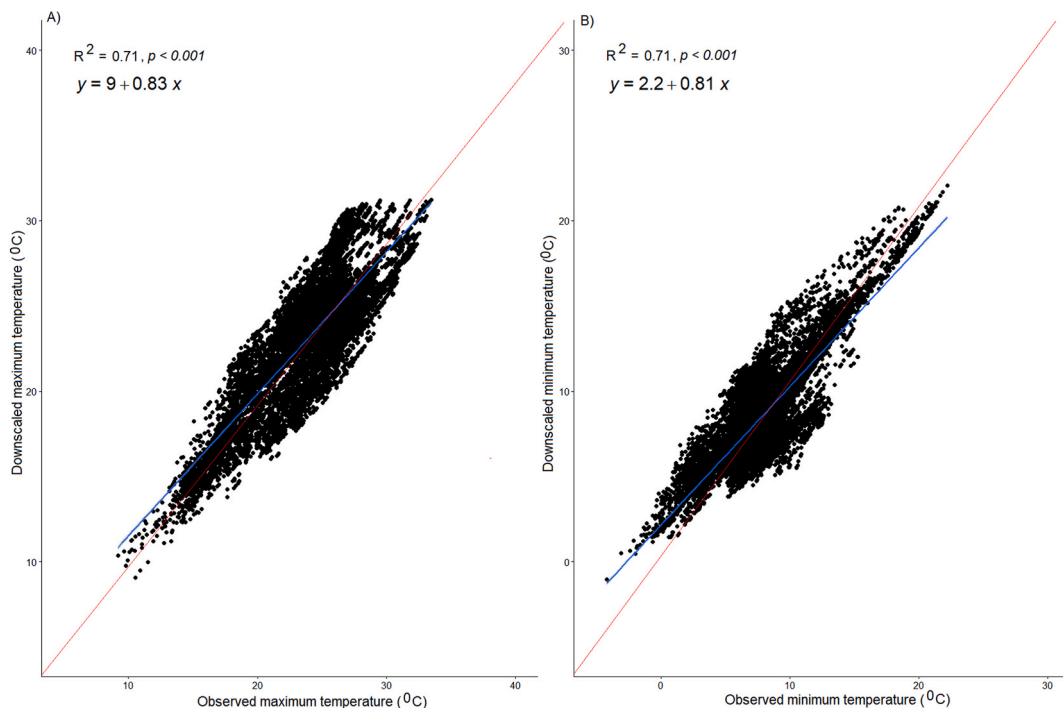


Fig. 3. Regression correlation with statistics between observed and downscaled values of maximum temperature (A), and minimum temperature (B) during the historical period.

3. Results and discussion

The regression correlation between the observed and downscaled maximum and temperature values is strong ($R^2 = 0.71$), with p values of <0.01 (Fig. 3). Fig. 4 compares the observed, original GCM, and downscaled CNNSD maximum and minimum temperature distributions over the historical period (1980–2014). CNNSD-downscaled temperatures showed less bias across the entire distribution, confirming the significance of climate downscaling-based deep learning. This indicates that the CNNSD model produced acceptable results in terms of representing observed values and the possibility of downscaling future climate change scenarios. Data in Figs. 5 and 6 show the mean daily downscaled maximum and minimum temperatures over the historical period (1980–2014), and future periods (2015–2100) for two SSPs and one GCM (CanESM5). The CNNSD model displayed a smooth spatial pattern of maximum and minimum temperatures over historical and future periods, in contrast to the original GCM values, which failed to capture local variability and overestimated temperature values (Supplementary Fig. 2). The CNNSD model exhibits a robust and unbiased spatial pattern of maximum and minimum temperature in Egypt, due to the direct training with observations. Similar findings in Europe demonstrated that statistical downscaling based on deep learning produces mostly smooth and unbiased spatial patterns that can be interpreted using the training process [58]. However, more research is needed to determine whether the difference between the original GCM and downscaled is due to the added value of downscaling or a model flaw. In terms of climate change in Egypt, based on downscaled temperatures under two SSPs over different periods, temperatures are expected to rise by the late century in SSP8.5 and SSP4.5 compared to the historical period.

For further analysis of downscaled scenarios and observation of maximum and minimum temperatures, Taylor diagrams were used (Fig. 7). This analysis is crucial for creating accurate future estimates [59,60]. In the case of maximum temperature (Fig. 7A), it was found that there are good correlations between observed values and SSP4.5 at the late period ($R^2 = 0.75$), SSP4.5 and SSP8.5 at the near time ($R^2 = 0.55$), while there was a weak correlation with SSP8.5 at the end of the century ($R^2 = 0.3$). In addition, the centered RMSE increased with SSP8.5 in the mid and late periods. The same trend was noticed with minimum temperature in all scenarios

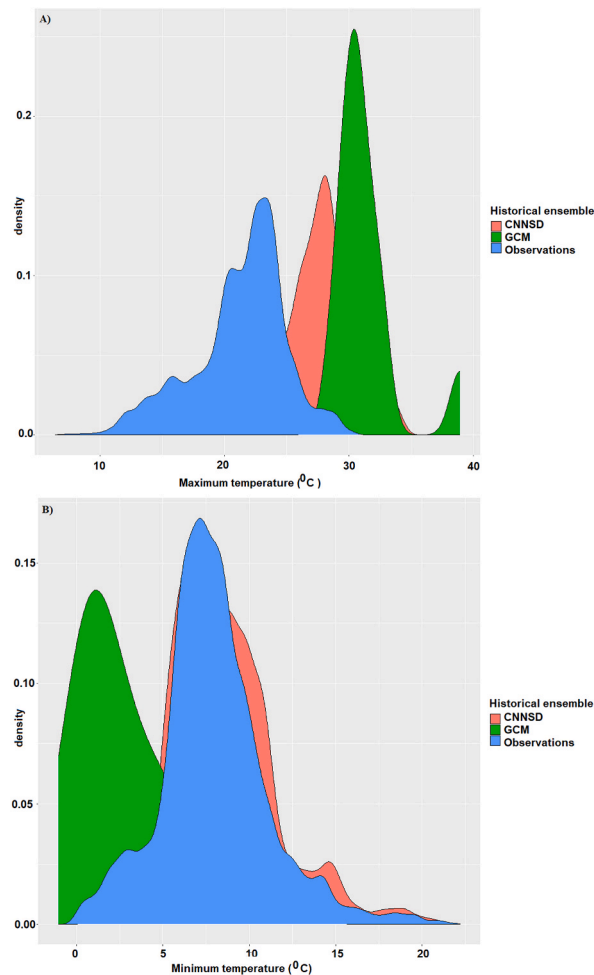


Fig. 4. Probability density distribution of observed, original GCM without downscaling, and downscaled by CNNSD maximum temperature (A) and minimum temperature (B) during the historical period (1980–2014).

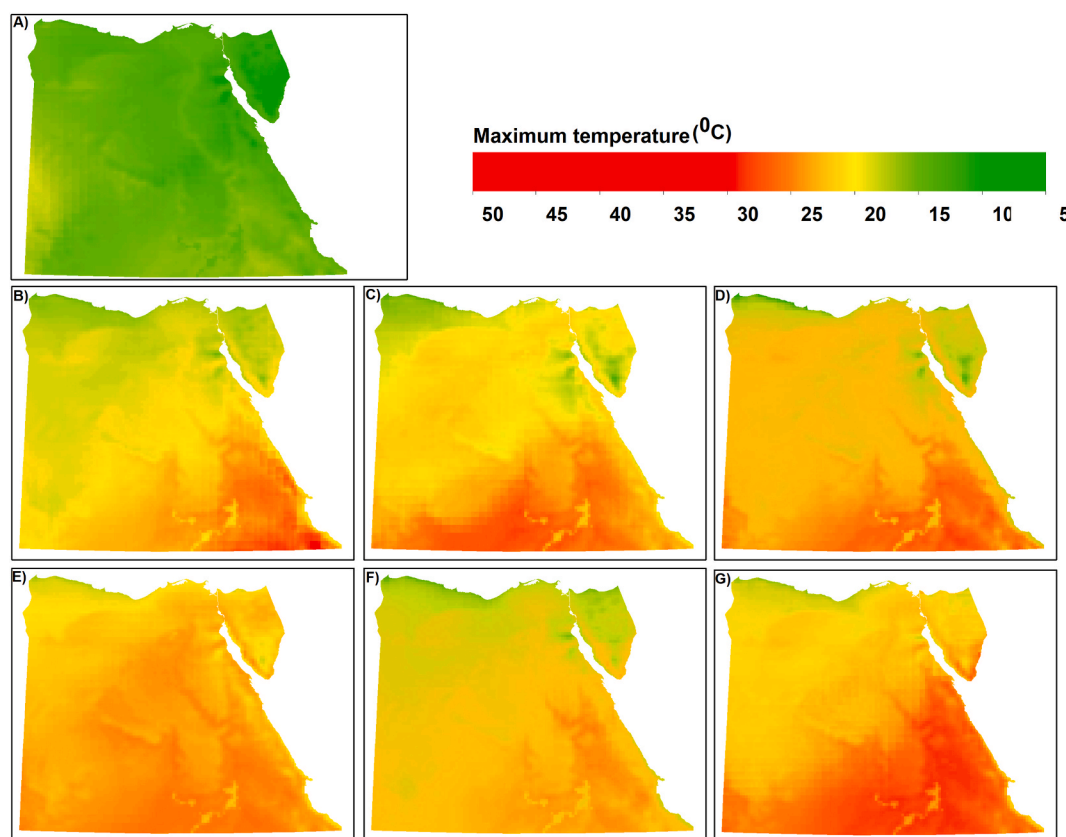


Fig. 5. Daily historical (A), and future downscaled maximum temperature as obtained from the GCM (CanESM5) downscaled the CNNSD algorithm. The future periods are near-term (B and E), mid-term (C and F), and late-term (D and G) under SSP4.5 (B,C, and D), and business as usual, SSP8.5 (E, F, and G) scenarios.

(Fig. 7B). Although there are some correlations between observed and downscaled temperatures at various scenarios and periods ($R^2 = 0.3\text{--}0.75$), they appear to be not strong, which may be due to the use of a single GCM with different SSPs. Furthermore, CanESM5 has a significantly higher equilibrium climate sensitivity than its predecessor [61]. More GCMs may result in higher correlations than a single GCM, necessitating further research into the use of multi-GCMs in the region. Various studies have shown that combining different GCMs is much better because it reduces uncertainty [62,63]. Furthermore, GCMs are regarded as a major source for investigating climate complexity and providing quantitative estimates of future climate change.

Boxplots in S. Fig. 5A showed that the average maximum temperature will increase from 25 °C in the historical period to 32 °C and 35 °C for SSP4.5 and SSP8.5 respectively. The same trend was found in the minimum temperature, which was expected to rise from 7 °C in the historical period to 18 °C in the case of SSP4.5, and 21 °C in the case of SSP8.5 (S. Fig. 5B). The uncertainty appears to be higher in SSP8.5 than in SSP4.5 and historical, as well as in the late century as opposed to the mid and near. This is because SSP4.5 (Middle of the Road) represents moderate challenges to both mitigation and adaptation, whereas SSP8.5 (Fossil-fueled Development) represents high mitigation challenges and low adaptation challenges. Both scenarios showed an increase in the expected future maximum and minimum temperatures relative to the historical period (Fig. 8). The maximum temperature increase is projected to be 4.2, 4.0, and 6.1 °C under SSP4.5; 6.3, 6.1, and 6.5 with SSP8.5 for near, mid, and late periods respectively (Fig. 8A). Meanwhile, the minimum temperature is expected to increase by 3.7, 4.1, and 4.2 °C under SSP4.6, and 4.3, 4.1, and 4.4 °C under SSP8.5 for near, mid, and late periods respectively. This increase is also consistent with what is described in the IPCC's sixth assessment report (AR6) when the CanSM5 model is used.

The CNN model's downscaling of maximum and minimum temperatures in Egypt produced consistent results across periods, scenarios, and with a single GCM. However, more research is needed to include multi-GCMs to improve the outputs for use in climate change impacts and adaptations for food security. This will enable deploying multi-climate models [64], and multi-scenario analysis in arid to semi-arid climatic conditions. Furthermore, another significant variable for predicting crop growth in a certain climate is radiation use efficiency [65], which is a vital element of radiation-based crop growth models and should be incorporated alongside temperatures in future downscaling. The developed approach could be used not only in Egypt but also in the MENA region, which is particularly vulnerable to climate change and suffers from a lack of related research.

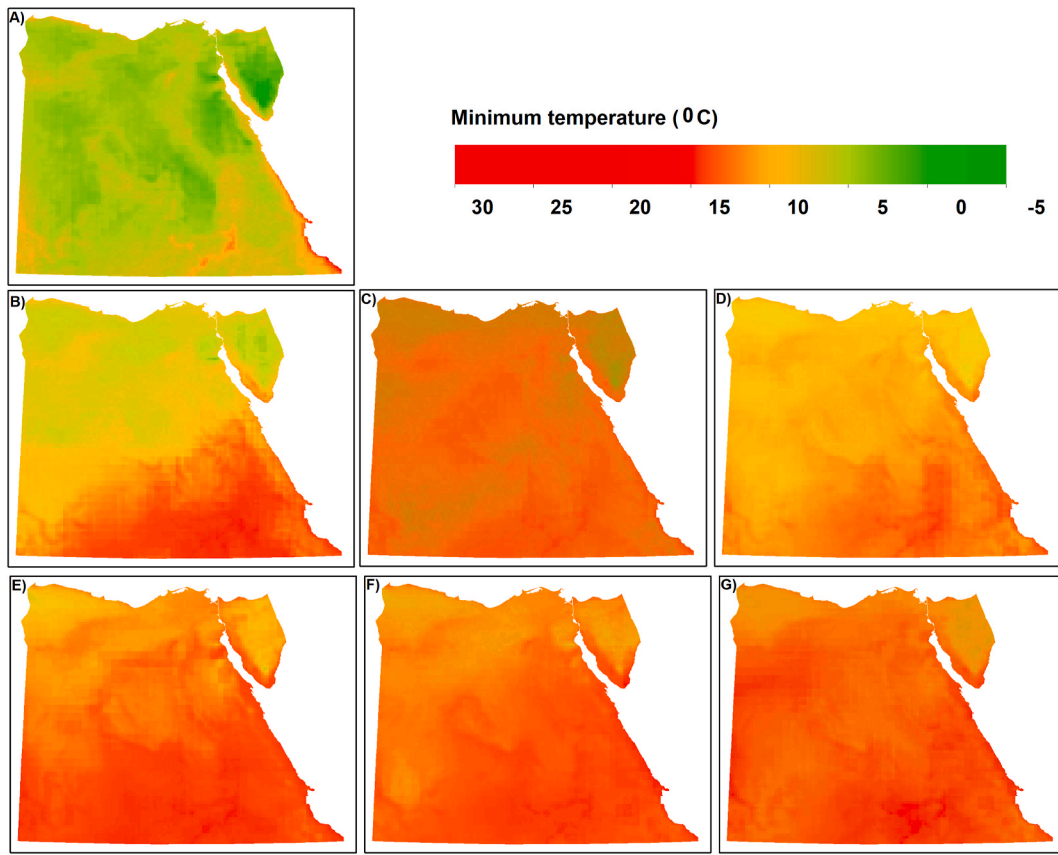


Fig. 6. Daily historical (A), and future downscaled minimum temperature as obtained from the GCM (CanESM5) downscaled by the CNNSD algorithm. The future periods are near-term (B and E), mid-term (C and F), and late-term (D and G) under SSP4.5 (B, C, and D), and business as usual, SSP8.5 (E,F, and G) scenarios.

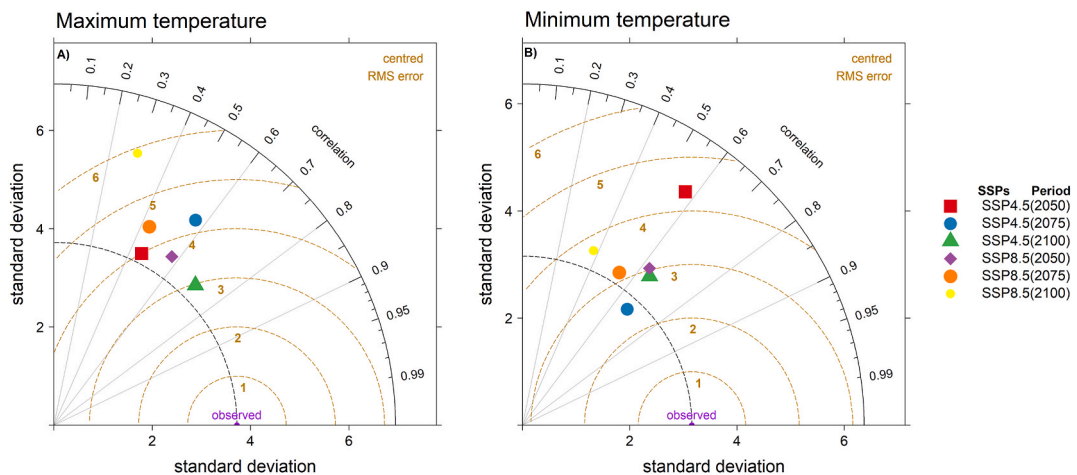


Fig. 7. Taylor diagram of downscaled maximum temperature (A), and minimum temperature (B) for observed (historical) and each SSP scenario under CanESM5 (future) in three time periods (2050, 2075, and 2100).

4. Conclusion

Due to their capacity to predict complicated non-linear patterns from climate data, deep learning topologies are being investigated for downscaling purposes more and more. These tests show promising outcomes in the current environment. Yet, there are still

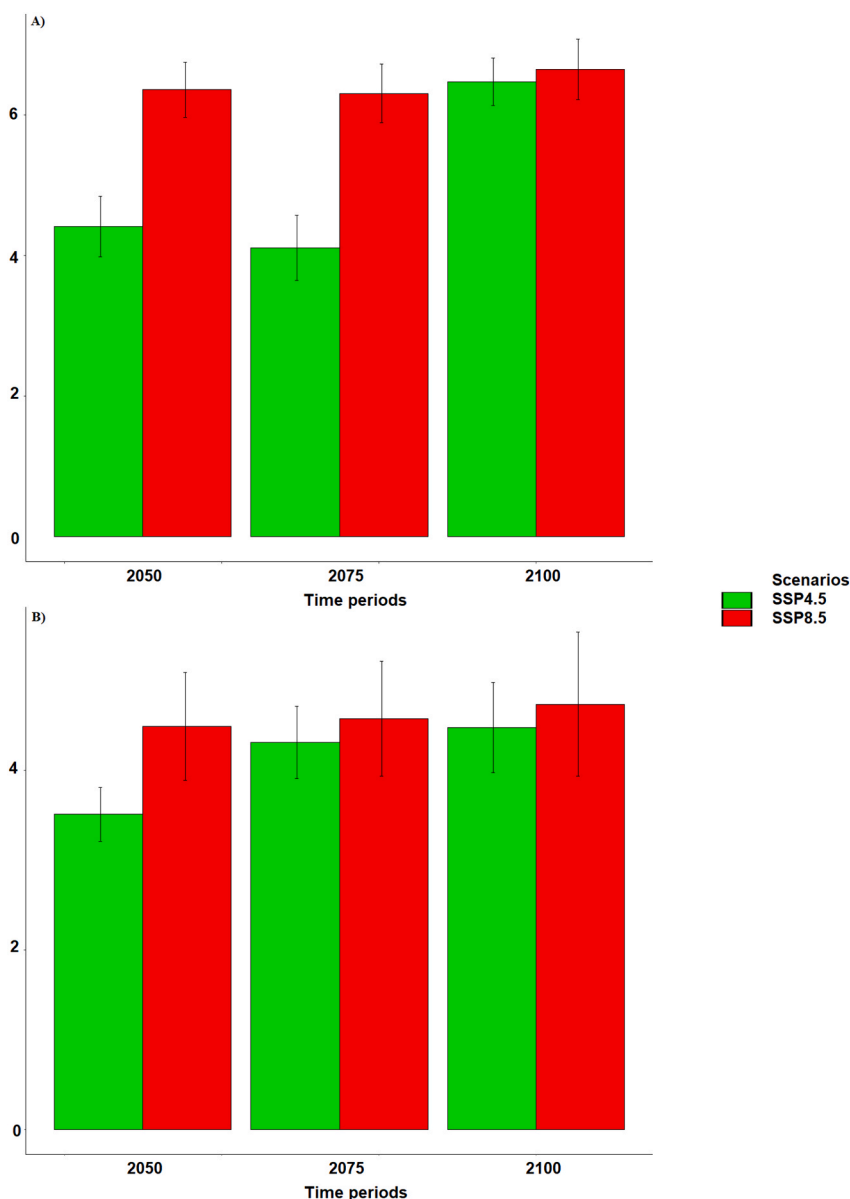


Fig. 8. Changes of downscaled future maximum temperature (A), and minimum temperature (B) during 2050, 2075, and 2100 under the GCM (CanESM5) and two SSPs relative to the historical values (1980–2014) using CNNSD. The bars are mean, and the error bars are standard deviation.

numerous unanswered questions about how well these models can be generalized to climate scenarios in coarse resolution, particularly in arid regions. We used the CNNSD model to downscale maximum and minimum temperatures over Egypt in historical (1980–2014) and future (2050, 2075, and 2100) periods using one GCM and two SSPs (SSP4.5 and SSP8.5). The downscaled maximum and minimum temperature-based CNN was able to reproduce the observed climate at a distributional level over historical and future periods, reducing the biases exhibited by the GCM. Although this is the first study using statistical downscaling-based deep learning in Egypt as an arid region, further research is needed to use multi-GCMs in the CNN model to quantify the uncertainties between GCMs and SSPs. This will increase the potential of using downscaled variables in crop models not only in Egypt but also in similar arid environments throughout the MENA region and developing countries.

Author contribution statement

Ahmed Kheir and Ajit Govind: Conceived and designed; Analyzed and interpreted the data. </p>

Alaa Mosaad and Abdelrazek Elnashar: Performed the experiments. </p>

Ahmed Kheir: Contributed reagents, materials, analysis tools or data. </p>

Ahmed Kheir, AE, Alaa Mosaad, Ajit Govind and Abdelrazek Elnashar: Wrote the paper. </p>

Data availability statement

Data will be made available on request.

Declaration of competing interest

The authors declare that they have no known competing financial interests or personal relationships that could have appeared to influence the work reported in this paper.

Acknowledgements

Authors acknowledge the CGIAR Excellence in Agronomy-Egypt Use Case (<https://www.cgiar.org/initiative/11-excellence-in-agronomy-eia-solutions-for-agricultural-transformation>). We also sincerely acknowledge the CGIAR-INIT-23: Building Systemic Resilience Against Climate Variability and Extreme (*ClimBeR* project), (Grant Number 200303) for funding.

Appendix A. Supplementary data

Supplementary data to this article can be found online at <https://doi.org/10.1016/j.heliyon.2023.e18200>.

References

- [1] S. Asseng, et al., Climate change impact and adaptation for wheat protein, *Global Change Biol.* 25 (1) (2019) 155–173.
- [2] M.G.M. Ali, et al., Climate change impact and adaptation on wheat yield, water use and water use efficiency at North Nile Delta, *Front. Earth Sci.* 14 (3) (2020) 522–536.
- [3] A.M.S. Kheir, et al., Impacts of rising temperature, carbon dioxide concentration and sea level on wheat production in North Nile delta, *Sci. Total Environ.* 651 (2019) 3161–3173.
- [4] G. Abbas, et al., Global framework on climate change, in: W.N. Jatoi, et al. (Eds.), *Climate Change Impacts on Agriculture: Concepts, Issues and Policies for Developing Countries*, Springer International Publishing, Cham, 2023, pp. 3–22.
- [5] M. Mubeen, et al., Evaluating the climate change impact on water use efficiency of cotton-wheat in semi-arid conditions using DSSAT model, *J. Water Clim. Change* 11 (4) (2019) 1661–1675.
- [6] S. Hussain, et al., Spatiotemporal variation in land use land cover in the response to local climate change using multispectral remote sensing data, *Land* 11 (5) (2022) 595.
- [7] M. Tariq, et al., The impact of climate warming and crop management on phenology of sunflower-based cropping systems in Punjab, Pakistan, *Agric. For. Meteorol.* 256–257 (2018) 270–282.
- [8] K.E. Taylor, R.J. Stouffer, G.A. Meehl, An overview of CMIP5 and the experiment design, *Bull. Am. Meteorol. Soc.* 93 (4) (2012) 485–498.
- [9] S. Ali, et al., Assessment of climate extremes in future projections downscaled by multiple statistical downscaling methods over Pakistan, *Atmos. Res.* 222 (2019) 114–133.
- [10] V. Eyring, et al., Overview of the coupled model intercomparison project phase 6 (CMIP6) experimental design and organization, *Geosci. Model Dev. (GMD)* 9 (5) (2016) 1937–1958.
- [11] G.A. Meehl, et al., Overview of the coupled model intercomparison project, *Bull. Am. Meteorol. Soc.* 86 (1) (2005) 89–93.
- [12] J.-Y. Lee, B. Wang, Future change of global monsoon in the CMIP5, *Clim. Dynam.* 42 (1) (2014) 101–119.
- [13] C.-w. Zheng, et al., Projection of future global offshore wind energy resources using CMIP data, *Atmos.-Ocean* 57 (2) (2019) 134–148.
- [14] C. Müller, et al., Exploring uncertainties in global crop yield projections in a large ensemble of crop models and CMIP5 and CMIP6 climate scenarios, *Environ. Res. Lett.* 16 (3) (2021), 034040.
- [15] J. Li, et al., Comparative assessment and future prediction using CMIP6 and CMIP5 for annual precipitation and extreme precipitation simulation, *Front. Earth Sci.* 9 (2021).
- [16] M.S. Shiru, J.H. Kim, E.-S. Chung, Variations in projections of precipitations of CMIP6 global climate models under SSP 2–45 and SSP 5–85, *KSCE J. Civ. Eng.* 26 (12) (2022) 5404–5416.
- [17] A. Mehran, A. AghaKouchak, T.J. Phillips, Evaluation of CMIP5 continental precipitation simulations relative to satellite-based gauge-adjusted observations, *J. Geophys. Res. Atmos.* 119 (4) (2014) 1695–1707.
- [18] T.H.J. Hermans, et al., Projecting global mean sea-level change using CMIP6 models, *Geophys. Res. Lett.* 48 (5) (2021), e2020GL092064.
- [19] H.M. Sung, et al., Future changes in the global and regional sea level rise and sea surface temperature based on CMIP6 models, *Atmosphere* 12 (2021), <https://doi.org/10.3390/atmos12010090>.
- [20] S. Zhao, et al., Evaluation of the performance of CMIP5 models to simulate land surface air temperature based on long-range correlation, *Front. Environ. Sci.* 9 (2021).
- [21] D. Carvalho, et al., How well have CMIP3, CMIP5 and CMIP6 future climate projections portrayed the recently observed warming, *Sci. Rep.* 12 (1) (2022), 11983.
- [22] S. Kamworapan, C. Surussavadee, Evaluation of CMIP5 global climate models for simulating climatological temperature and precipitation for Southeast Asia, *Adv. Meteorol.* 2019 (2019), 1067365.
- [23] J. Zhai, et al., Future drought characteristics through a multi-model ensemble from CMIP6 over South Asia, *Atmos. Res.* 246 (2020), 105111.
- [24] A. Srivastava, R. Grotjahn, P.A. Ullrich, Evaluation of historical CMIP6 model simulations of extreme precipitation over contiguous US regions, *Weather Clim. Extrem.* 29 (2020), 100268.
- [25] I.K. Nooni, et al., Future changes in simulated evapotranspiration across continental Africa based on CMIP6 CNRM-CM6, *Int. J. Environ. Res. Publ. Health* 18 (13) (2021).
- [26] F. Fuso Nerini, et al., Connecting climate action with other sustainable development goals, *Nat. Sustain.* 2 (8) (2019) 674–680.
- [27] H. Dannevig, M.H. Korsbrette, G.K. Hovelsrud, Advancements of sustainable development goals in co-production for climate change adaptation research, *Clim. Risk Manag.* 36 (2022), 100438.

- [28] A. Elnashar, et al., Downscaling TRMM monthly precipitation using google earth engine and google cloud computing, *Rem. Sens.* 12 (23) (2020) 3860.
- [29] W. Immerzeel, M. Rutten, P. Droogers, Spatial downscaling of TRMM precipitation using vegetative response on the Iberian Peninsula, *Rem. Sens. Environ.* 113 (2) (2009) 362–370.
- [30] Z. Duan, W.G.M. Bastiaanssen, First results from version 7 TRMM 3B43 precipitation product in combination with a new downscaling-calibration procedure, *Rem. Sens. Environ.* 131 (2013) 1–13.
- [31] A. Elnashar, et al., Soil erosion assessment in the Blue Nile Basin driven by a novel RUSLE-GEE framework, *Sci. Total Environ.* 793 (2021), 148466.
- [32] C. Teutschbein, F. Wetterhall, J. Seibert, Evaluation of different downscaling techniques for hydrological climate-change impact studies at the catchment scale, *Clim. Dynam.* 37 (9) (2011) 2087–2105.
- [33] P. López López, et al., Spatial downscaling of satellite-based precipitation and its impact on discharge simulations in the Magdalena river basin in Colombia, *Front. Earth Sci.* 6 (68) (2018).
- [34] S. Jia, et al., A statistical spatial downscaling algorithm of TRMM precipitation based on NDVI and DEM in the Qaidam Basin of China, *Rem. Sens. Environ.* 115 (12) (2011) 3069–3079.
- [35] J. Fang, et al., Spatial downscaling of TRMM precipitation data based on the orographical effect and meteorological conditions in a mountainous area, *Adv. Water Resour.* 61 (2013) 42–50.
- [36] W. Jing, et al., A comparison of different regression algorithms for downscaling monthly satellite-based precipitation over North China, *Rem. Sens.* 8 (10) (2016) 835.
- [37] J. Baño-Medina, et al., *Downscaling multi-model climate projection ensembles with deep learning (DeepESD): contribution to CORDEX EUR-44*, *Geosci. Model Dev.* 15 (17) (2022) 6747–6758.
- [38] N. Rampal, et al., High-resolution downscaling with interpretable deep learning: rainfall extremes over New Zealand, *Weather Clim. Extrem.* 38 (2022), 100525.
- [39] A. Amin, et al., Evaluation and analysis of temperature for historical (1996–2015) and projected (2030–2060) climates in Pakistan using SimCLIM climate model: ensemble application, *Atmos. Res.* 213 (2018) 422–436.
- [40] W. Nasim, et al., Future risk assessment by estimating historical heat wave trends with projected heat accumulation using SimCLIM climate model in Pakistan, *Atmos. Res.* 205 (2018) 118–133.
- [41] Ojha, M.K.G.a.C.S.P., Robust weighted regression as a downscaling tool in temperature projections, *Int. J. Glob. Warming* 2 (3) (2010) 234–251.
- [42] C.S.P.O. Manish Kumar Goyal, Evaluation of various linear regression methods for downscaling of mean monthly precipitation in arid Pichola watershed, *Nat. Resour.* 1 (2010) 11–18.
- [43] M.K. Goyal, C.S.P. Ojha, Downscaling of precipitation on a lake basin: evaluation of rule and decision tree induction algorithms, *Nord. Hydrol* 43 (3) (2012) 215–230.
- [44] W.T. Anna Vaughan, J. Scott Hosking, Richard E. Turner, Convolutional conditional neural processes for local climate downscaling, *Geosci. Model Dev. (GMD)* (2021), <https://doi.org/10.5194/gmd-2020-420>.
- [45] K. Höhle, et al., A comparative study of convolutional neural network models for wind field downscaling, *Meteorol. Appl.* 27 (6) (2020) e1961.
- [46] J. Baño-Medina, R. Manzananas, J.M. Gutiérrez, Configuration and intercomparison of deep learning neural models for statistical downscaling, *Geosci. Model Dev. (GMD)* 13 (4) (2020) 2109–2124.
- [47] M.M. Hamed, M.S. Nashwan, S. Shahid, Climatic zonation of Egypt based on high-resolution dataset using image clustering technique, *Prog. Earth Planet. Sci.* 9 (1) (2022) 35.
- [48] H. Hersbach, et al., The ERA5 global reanalysis, *Q. J. R. Meteorol. Soc.* 146 (730) (2020) 1999–2049.
- [49] D. Maraun, M. Widmann, *Statistical Downscaling and Bias Correction for Climate Research*, Cambridge University Press, Cambridge, 2018.
- [50] M. Mateen, et al., Fundus image classification using VGG-19 architecture with PCA and SVD, *Symmetry* 11 (1) (2018) 1.
- [51] C. Chaudhuri, C. Robertson, CliGAN: a structurally sensitive convolutional neural network model for statistical downscaling of precipitation from multi-model ensembles, *Water* 12 (12) (2020) 3353.
- [52] R. Yamashita, et al., Convolutional neural networks: an overview and application in radiology, *Insights Imag.* 9 (4) (2018) 611–629.
- [53] S.F. Ahmed, et al., Deep Learning Modelling Techniques: Current Progress, Applications, Advantages, and Challenges, *Artificial Intelligence Review*, 2023.
- [54] O. Bazgir, et al., Representation of features as images with neighborhood dependencies for compatibility with convolutional neural networks, *Nat. Commun.* 11 (1) (2020) 4391.
- [55] J. Bedia, et al., Statistical downscaling with the downscaleR package (v3.1.0): contribution to the VALUE intercomparison experiment, *Geosci. Model Dev. (GMD)* 13 (3) (2020) 1711–1735.
- [56] J. Baño-Medina, Understanding deep learning decisions in statistical downscaling models, in: *Proceedings of the 10th International Conference on Climate Informatics, Association for Computing Machinery: virtual, United Kingdom*, 2021, pp. 79–85.
- [57] M. Vrac, P. Vaittinada Ayar, Influence of bias correcting predictors on statistical downscaling models, *J. Appl. Meteorol. Climatol.* 56 (1) (2017) 5–26.
- [58] Gutierrez, A.C.S.H.J.F.J.M., Towards a fair comparison of statistical and dynamical downscaling in the framework of the EURO-CORDEX initiative, *Climatic Change* 137 (2016) 411–426.
- [59] R. Knutti, Why are climate models reproducing the observed global surface warming so well? *Geophys. Res. Lett.* 35 (18) (2008).
- [60] D.J. Peres, et al., Evaluation of EURO-CORDEX (Coordinated Regional Climate Downscaling Experiment for the Euro-Mediterranean area) historical simulations by high-quality observational datasets in southern Italy: insights on drought assessment, *Nat. Hazards Earth Syst. Sci.* 20 (11) (2020) 3057–3082.
- [61] N.C. Swart, et al., The Canadian earth system model version 5 (CanESM5.0.3), *Geosci. Model Dev. (GMD)* 12 (11) (2019) 4823–4873.
- [62] N. Acharya, et al., Development of an artificial neural network based multi-model ensemble to estimate the northeast monsoon rainfall over south peninsular India: an application of extreme learning machine, *Clim. Dynam.* 43 (2014) 1303–1310.
- [63] G. Wang, M. Yu, Y. Xue, Modeling the potential contribution of land cover changes to the late twentieth century Sahel drought using a regional climate model: impact of lateral boundary conditions, *Clim. Dynam.* 47 (2016) 3457–3477.
- [64] M.H.u. Rahman, et al., Multi-model projections of future climate and climate change impacts uncertainty assessment for cotton production in Pakistan, *Agric. For. Meteorol.* 253–254 (2018) 94–113.
- [65] M.H. ur Rahman, et al., Influence of semi-arid environment on radiation use efficiency and other growth attributes of lentil crop, *Environ. Sci. Pollut. Control Ser.* 28 (11) (2021) 13697–13711.